

UNIVERSITÀ DEGLI STUDI DI PADOVA

Dipartimento di Ingegneria Industriale

Corso di Laurea Magistrale in Ingegneria Energetica

Tesi di Laurea

**Techno-economic analysis of a mechanical vapor  
compression desalination system for volume  
minimization of reverse osmosis brine**

Relatore: Prof. Andrea Lazzaretto

Supervisors: Dr. Michele Stefani

Dr. Florent Cesarole

Andrea Randon 1108696

Anno accademico 2018/2019



# Abstract

In all desalination plants the brine disposal is a matter of concern, representing an environmental and economic issue. In particular, the volume of the concentrate is becoming one of the main drawback of the reverse osmosis process. Brine minimization using either membrane or thermal processes is one of the strategies adopted to manage the problem. The present study is focused on the development of a techno-economic analysis of a Single Effect-Mechanical Vapor Compression (SE-MVC) system for purposes of brine volume minimization. The aim is to evaluate the performances as well as the capital and operating expenditures of the brine concentrator when being part of a near zero liquid discharge (near-ZLD) application. This is achieved by developing the thermodynamic and economic models of the system, which are then combined together in a single integrated procedure. Brackish water analysis is used as starting point for this work. Water properties are modeled using Pitzer's equations as well as correlations found in the literature. The evaporator model provides the necessary input variables for the economic model. For a feed flow of  $10.147 \frac{kg}{s}$  and an heat duty of  $18080 kW$ , the capital cost of equipment is  $1119.7 k\text{€}y^{-1}$ , while the operational expenses are  $641.1 k\text{€}y^{-1}$ . The total annualized cost of the process is  $1760.8 k\text{€}y^{-1}$ .

# Sommario

In tutti gli impianti di dissalazione lo smaltimento delle salamoie è motivo di preoccupazione, rappresentando un problema ambientale ed economico. In particolare, il volume del concentrato sta diventando uno dei maggiori inconvenienti del processo di osmosi inversa. Una delle strategie principali è la riduzione al minimo del volume della salamoia che utilizza processi a membrana o termici. Il presente studio è incentrato sullo sviluppo di un'analisi tecnico-economica di un sistema a singolo effetto con compressione meccanica del vapore (SE-MVC) per scopi di minimizzazione del volume della salamoia. Lo scopo è quello di valutare le prestazioni nonché le spese di capitale e di esercizio del concentratore di salamoia quando facente parte di un'applicazione vicina allo zero scarico di liquido (near-ZLD). L'obiettivo si è ottenuto sviluppando i modelli termodinamici ed economici del sistema combinandoli poi insieme in un'unica procedura integrata. Analisi di acqua salmastra sono utilizzate come punto di partenza per questo lavoro. Le proprietà dell'acqua sono modellate usando le equazioni del modello di Pitzer, come anche correlazioni trovate in letteratura. Il modello dell'evaporatore fornisce le variabili di input necessarie per il modello economico. Per un flusso di alimentazione di  $10.147 \frac{kg}{s}$  e un consumo di calore di  $18080 kW$ , il costo di investimento delle attrezzature è di  $1119,7 k\text{€}y^{-1}$ , mentre le spese operative sono  $641,1 k\text{€}y^{-1}$ . Il costo totale annualizzato del sistema è  $1760,8 k\text{€}y^{-1}$ .

# Contents

|  |            |
|--|------------|
| <b>Abstract</b>  | <b>iii</b> |
| <b>Sommario</b>  | <b>iv</b>  |
| <b>Contents</b>  | <b>v</b>   |
| <b>List of Figures</b>   | <b>vii</b> |
| <b>List of Tables</b>  | <b>ix</b>  |
| <b>Acknowledgements</b>  | <b>xi</b>  |
| <b>Introduction</b>  | <b>1</b>   |
| <b>1 Thermal Brine Minimization Systems</b>  | <b>5</b>   |
| 1.1 Multiple-Effect Distillation (MED) . . . . .                                   | 6          |
| 1.2 Mechanical Vapor Compression (MVC) . . . . .                                   | 7          |
| 1.3 Humidification De-Humidification (HDH) . . . . .                               | 8          |
| 1.4 Membrane Distillation (MD) . . . . .   | 9          |
| 1.5 Eutectic Freeze Crystallization (EFC) . . . . .                                | 10         |
| <b>2 The Mechanical Vapor Compression system for the brine volume minimization</b> | <b>11</b>  |
| 2.1 Process Description . . . . .  | 12         |
| <b>3 Methods</b>   | <b>15</b>  |
| 3.1 Electrolytes solutions thermodynamics - Pitzer model . . . . .                 | 15         |

|  |           |
|--|-----------|
| Electrolytes solutions thermodynamics - Pitzer model . . . . .                   | 15        |
| 3.2 Thermodynamic model of the MVC brine minimization system . . . . .           | 17        |
| 3.3 Economic model . . . . .   | 20        |
| 3.3.1 Fixed Costs . . . . .  | 20        |
| 3.3.2 Operating Costs . . . . .  | 21        |
| <b>4 Results</b>   | <b>23</b> |
| <b>5 Conclusions</b>   | <b>27</b> |
| <b>Appendices</b>  | <b>29</b> |
| <b>A Pitzer equations and parameters</b>   | <b>29</b> |
| <b>B Thermodynamic model - Single Effect Mechanical Vapor Compression system</b> | <b>32</b> |
| <b>Bibliography</b>  | <b>35</b> |

# List of Figures

|     |  |    |
|-----|--|----|
| 1.1 | Schematic of a Multiple-Effect Distillation system . . . . .   | 6  |
| 1.2 | Schematic of a Mechanical Vapor Compression system . . . . .   | 7  |
| 1.3 | Simplest scheme of a Humidification De-Humidification cycle . . . . .  | 8  |
| 1.4 | Schematic of a Direct Contact Membrane Distillation unit with temperature profile . . . . .  | 9  |
| 2.1 | (a) Evaporator temperature profiles (b) T-s diagram . . . . .  | 11 |
| 2.2 | Process Flowsheet . . . . .  | 12 |
| 4.1 | Influence of molality and temperature on the Boiling Point Elevation. . .  | 24 |
| 4.2 | (a) Influence of the temperature difference on the specific power consumption and the heat transfer area. (b) Comparative effect of produced water salinity on the specific heat transfer area and recovery ratio. . . . . | 24 |
| 4.3 | (a) Effect of increasing the salinity of feed water on capital and operational expenditure. (b) Effect of increasing the salinity of feed water total annualized cost and simplified cost of water. . . . .                | 25 |





# List of Tables

|     |                                 |    |
|-----|---------------------------------|----|
| 3.1 | BWRO reject quality . . . . .   | 16 |
| 3.2 | Indipendent variables . . . . . | 18 |
| 3.3 | Economic Parameters . . . . .   | 20 |



# Acknowledgements

I want to express my deepest gratitude to my parents and my brother, for the support and the encouragement that they always gave me, and for having always believed in me. Without them I would never been able to do this experience. I would also like to express my sincere appreciation to Prof. Andrea Lazzaretto for inspiring discussions and for the precious advices he gave me. Finally, I would like to thank Lenntech B.V., as well as Michele Stefani and Florent Cesarole for helpful discussions and suggestions, and for teaching me how to manage a project all by myself.



# Introduction

Fresh water availability is gradually decreasing and may limit the primary needs of drinking water and irrigation, as well as other activities, such as energy conversion, tourism, etc. A high number of desalination plants are being built to provide clean water. However, brine disposal represents both an environmental and an economic issue. So, it has to be taken into consideration from the beginning of the design process of a new desalination plant. The focus is here on brackish-water reverse osmosis plants where the volume of the concentrate has become the main drawback. Among the several characteristics which render it harmful there are high salinity (and density) values, presence of ions or heavy metals and, in case of thermal processes, an elevated discharge temperature. The amount of brine in inland reverse osmosis plants is even more difficult to be disposed. Until recently, the common practice was either to discharge the brine into the sea or watercourses, directly dispose it into a water body or to inject it in an inland well. The high penalties to be paid for discharging brine in surface water have become the driving force in the search for more sustainable options. The following main strategies have been developed to face the problem:

1. brine volume minimization, either through membrane or thermal technologies,
2. improved direct disposal,
3. reuse applications of reject brine.

The present study focuses on option 1), with specific attention to the development of a techno-economic analysis of a Single Effect Mechanical Vapor Compression (SE-MVC) evaporator. The process aims at concentrating the solution, by lowering the volume of the concentrate through evaporation of the solvent. When dealing with harsh feed water qualities, membrane processes are mainly limited by osmotic pressure and scale formation.

Attempting to overcome these problems leads to thermal processes that are more suitable to the treatment of such waters. In spite of the high costs, its advantage in this field often overcome economic issues. An alternative solution to treat the brine could be the development of hybrid plants, which use a combination of different desalination processes, either thermal, membrane-based or both combined together. The definition of the most suitable processes and the process combination in a treatment chain depend on several factors, namely the rejected brine volume, chemical composition, geographical position of the plant, feasibility of the process in terms of capital and operating costs, availability of storage capacities and transportation of the brine [1]. Most of the authors have designed and compared different evaporative technologies. An important contribution was given by El-Dessouky and Ettouney [2], who develop the models of several evaporative processes involved in desalination, laying the groundwork for further developments. Subsequently, H. Ettouney [3] has provided new design features of the SE-MVC system. Both works refer to a limited concentration range of the solution, and do not consider the variation of the boiling point elevation (BPE) as function of the composition of the solution, which can influence the estimation of the energy consumption at high concentrations. Indeed, in these type of applications where the evaluation of the boiling point elevation is important, it is necessary to know the osmotic coefficient, which represents the key factor to understand the solvent behaviour in such concentrated conditions. To obtain it, Pitzer developed a system of equations to evaluate the thermodynamic properties of electrolytes starting from, and improving, the Debye-Hückel model and publishing useful numerical calculations for more realistic models [4,5]. More recently, other authors have provided the basis for further developments of desalination technologies for high salinity waters. For example, Thiel et al. [6] analyze and compare the energy consumption of several desalination systems at the high salinities and diverse compositions commonly encountered in produced water from shale formations to guide the choice of the technology and address further system developments. In this context, Mechanical vapor compression (MVC) is considered one of the most established technologies, and it is widely deployed to treat high-salinity feeds [6]. They also investigate composition effects on scale formation [7]. Moreover, they find that Aqueous-NaCl solutions closely approximate natural seawater only for the typical seawater salinities and not for brackish waters ones [8]. Mistry et

al. [9] analyze the entropy generation mechanisms highlighting its importance in understanding the influence of the irreversibilities within the system on the required energy input. Lately, Chung et al. investigate the thermodynamic limits of the ZLD (Zero Liquid Discharge) process in the application to the state-of-the-art industrial processes; they conclude that, in terms of energy consumption, the brine concentration step has more potential for improvement than the crystallization step [10]. The final objective of the present paper is to estimate the CAPEX and OPEX of a Single Effect Mechanical Vapor Compressor system that minimizes the brine volume. Starting from a real water sample, the aim is reached by simulation runs of a model that (i) evaluates the boiling point elevation using the thermodynamic properties of aqueous electrolytes solutions (ii) defines the design of the system and (iii) performs the economic analysis.





# Chapter 1

## Thermal Brine Minimization Systems

Most desalination technologies do not usually achieve 100% water recovery. As a result, desalination plants produce vast volumes of brine wastes with many retained substances [21]. Different practices need to be followed to overcome the environmental issues linked to brine disposal by achieving higher water recovery from desalination processes. Thermal-based technologies typically utilized for RO concentrate treatment are evaporative, either mechanical or natural [19]. A commonly used thermal method for the management of brine is natural evaporation through the use of either evaporation ponds or wind-aided intensified evaporation (WAIV) [23]. Desalination by mean of evaporation are energy intensive [22], which resulted in the development of multiple-effect and vapor compression systems, which consume lower energy. Typical methods to reduce specific energy consumption for thermal systems are to use multiple effect configurations, such as multi-effect distillation (MED), thermal vapor compression (TVC) or mechanical vapor compression (MVC) [19]. The thermal efficiency of these evaporators are measured based on the gain output ratio (GOR), which is the ratio of mass of distillate produced to the mass of steam supplied to the system; the GOR is enhanced by the addition of a thermo-compressor between the cells to recycle the vapor and use it as heating media [19]. The higher the GOR, the more efficient the technology, producing more freshwater from the same amount of steam.

## 1.1 Multiple-Effect Distillation (MED)

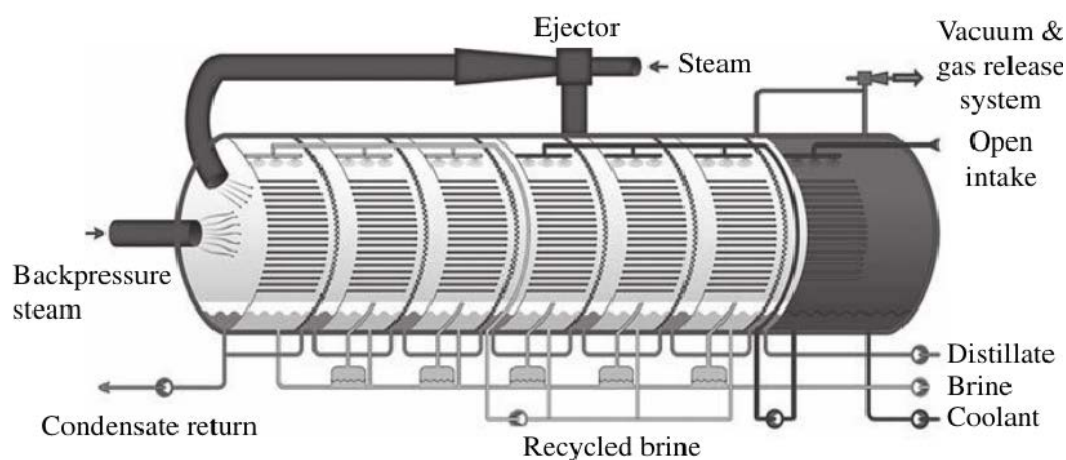


Figure 1.1: Schematic of a Multiple-Effect Distillation system

Other studies have shown the applicability of traditional thermal desalination approaches such as (multiple-effect distillation, MED) for the treatment of high-salinity reject brines. In MED, the evaporator consists of multiple cells operated at decreasing levels of pressure; the steam generated in one stage or effect is used to heat the concentrate in the next stage as the next stage is at a lower temperature or pressure. Heating steam is introduced inside the tubes and it condenses into distillate (fresh water) inside the tubes. At the same time the brine to be concentrated warms up and partly evaporates by recovering the latent heat released by the condensing steam. Due to evaporation brine slightly concentrates when flowing down the bundle and gives the by-product brine at the bottom of the cell. The vapor raised by evaporation is at a lower temperature than heating steam. However it can still be used as heating media for the next effect where the process is repeated. The decreasing pressure from one cell to the next one allows products to be drawn to the next cell where they will flash and release additional amounts of vapor at the lower pressure. This additional vapour will condense into distillate inside the next cell. This process is repeated in a series of effect (Multiple-Effect Distillation). In the last cell, the produced steam condenses on a conventional shell and tubes heat exchanger. This exchanger, called "distillate condenser" is cooled by the incoming brine. Brine and distillate are collected from cell to cell till the last one from where they are extracted by centrifugal pumps [27]. Its performance ratio (PR) depended on the number of stages/effects on the

system and water recovery from the RO-MED technique could reach 93%. To obtain a better outcome, thermo-compressor can be added as a heating media between the effects to recycle the vapor [20].

## 1.2 Mechanical Vapor Compression (MVC)

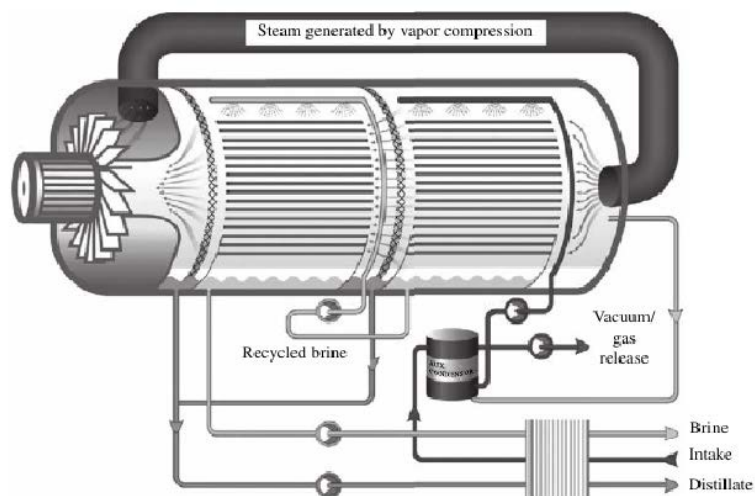


Figure 1.2: Schematic of a Mechanical Vapor Compression system

The Mechanical Vapor Compression (MVC) is among the most efficient distillation processes. It achieves its high efficiency in a simple manner, producing a high quality distillate. With this technology, vapor generated during evaporation is compressed using a mechanically driven compressor, which also acts as a heat pump, adding energy to the vapor. In such case the vapor is recycled from the cold cell to the hot one. After compression and condensation of the vapor, the pure water leaves the cycle separated from the vapor by the heat exchange surface of the evaporator [21]. MVC can be used to treat RO concentrate where distillate water and a more concentrated product are desired [19]. The system can be a useful solution for remote places because the energy input is the electrical power to drive the compressor, and therefore it is suitable for being coupled with renewable energy plants. This technology will be further investigated in this work.

### 1.3 Humidification De-Humidification (HDH)

Humidification-dehumidification (HDH) desalination involves vaporizing water from a saline liquid stream into a carrier gas stream and then condensing the vapor to form purified water. Nature uses air as a carrier gas to desalinate seawater by means of the rain cycle. In the rain cycle, seawater gets heated (by solar irradiation) and evaporates into the air above to humidify it. Then the humidified air rises and forms clouds. Eventually, the clouds de-humidify as rain and that which falls over land can be collected for human consumption. The man-made version of this cycle is called the humidification-dehumidification desalination (HDH) cycle. The simplest form of the HDH cycle is illustrated in figure 1.3. The HDH cycle has received some attention in recent years and many researchers have investigated the intricacies of this technology. It should be noted here that the predecessor technology of the HDH cycle is the simple solar still [1]. The main drawback of the solar still is that the various functional processes (solar absorption, evaporation, condensation, and heat recovery) all occur within a single component. By separating these functions into distinct components, thermal inefficiencies may be reduced and overall performance improved. This separation of functions is the essential characteristic of the HDH system [28].

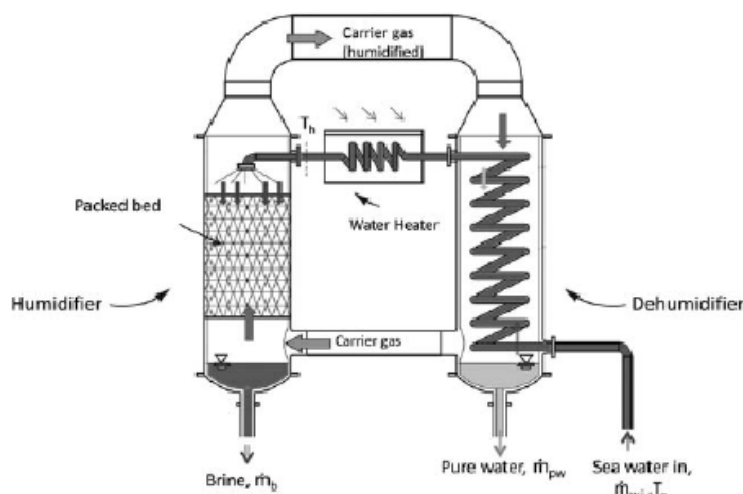


Figure 1.3: Simplest scheme of a Humidification De-Humidification cycle

## 1.4 Membrane Distillation (MD)

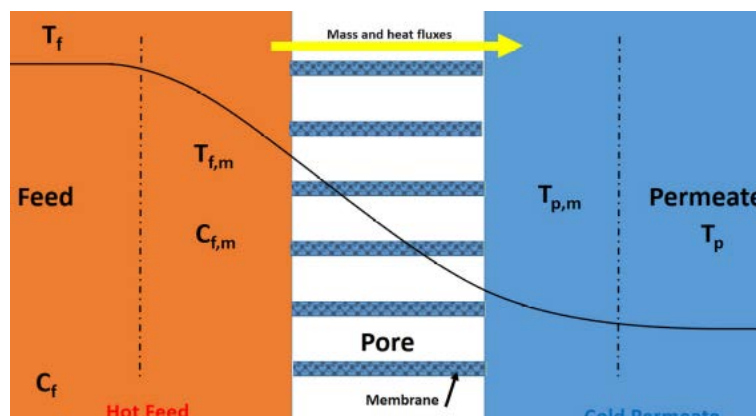


Figure 1.4: Schematic of a Direct Contact Membrane Distillation unit with temperature profile

Studies have also been carried out to investigate the potential of MD for the treatment of concentrated brine. MD combines both membranes and thermal technology [30]. It is an alternative process for the dewatering of highly concentrated aqueous solutions [30]. The driving force in MD is the vapor pressure gradient that can be produced by the temperature differential across the membrane [29, 31]. MD process is based on vapor–liquid equilibrium where volatile components diffuse across a micro-porous, hydrophobic membrane. MD technique has a potential for high water recovery from desalination concentrate. There are different configurations of MD such as direct contact, sweeping gas, air gap, and vacuum MD. The most convenient configuration unit that can be used for desalination purposes is direct contact MD (DCMD). On one side of the membrane in DCMD, the hot brine flows and the vapor is allowed to pass across the pores of the hydrophobic membrane. The vapor is then recovered as a cold distillate via condensation on the other side of the membrane. The concentrated phase containing more dissolved salts and other chemicals is retained by the hydrophobic membrane. The advantages of MD include: the vapor pressure driving force which is not considerably affected by high salt concentrations; low organic fouling and biofouling; ability to be coupled with different sources of heat like solar thermal, geothermal, or heat wasted from machines such as electrical and diesel generators and heat exchangers; and potentially low capital and operating cost requirements. The most common drawback of MD is the low permeate

flux achieved in many cases [20].

## 1.5 Eutectic Freeze Crystallization (EFC)

Desalination by freezing is categorized as a crystallization process. In this process, RO concentrate is frozen continuously until the eutectic temperature is reached [24]. Fernández-Torres et al. [25] proposed eutectic freeze crystallization (EFC) as an alternative to evaporative crystallization (EC) which is energy intensive and expensive. Further heat removal, beyond the eutectic temperature, resulted in both ice and salt crystallization. These ice crystals were washed and re-melted to obtain pure water. In a direct freezing process, the refrigerant is mixed directly with the concentrate. In an indirect process, the refrigerant is separated from the concentrate by a heat transfer surface [26]. It is possible to assimilate the process as a compressor-driven refrigeration cycle with the evaporator serving as the ice freezer, and the condenser as the ice melter. While desalination by freezing has been proposed as a method for several decades, only few pilot and demonstration projects have been conducted to date. Using EFC for treating RO concentrate (conductivity of 22 mS/cm), Randall et al. [26] demonstrated 97% conversion of concentrate as pure water with pure calcium sulfate (98.0% purity) and sodium sulfate salt products. When a life cycle assessment (LCA) was performed between EFC and EC for mine wastewater treatment, for a 4% (by mass) of  $\text{Na}_2\text{SO}_4$  solution, EFC was found to consume 6–7 times less energy when compared to EC [25].

# Chapter 2

## The Mechanical Vapor Compression system for the brine volume minimization

The thermal brine minimization system is based on the distillation process, in which we can identify four main streams: the feed water to be concentrated; the generated steam, which is compressed and then used as a source of heat; distilled water and concentrate as products. Figure 1.1b) shows the thermodynamic processes involved in the distillation process in the T-s diagram: after preheating the subcooled feed water (2 – 2'), the evaporation (2' – 3) generates water vapor which is then compressed (3 – 4) to allow the subsequent condensation (4' – 5) and release the necessary heat for the evaporation in order to continue the concentration process.

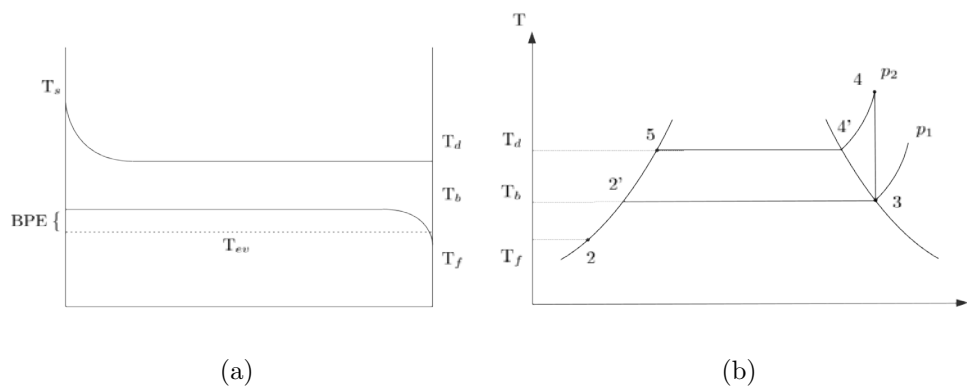


Figure 2.1: (a) Evaporator temperature profiles (b) T-s diagram

## 2.1 Process Description

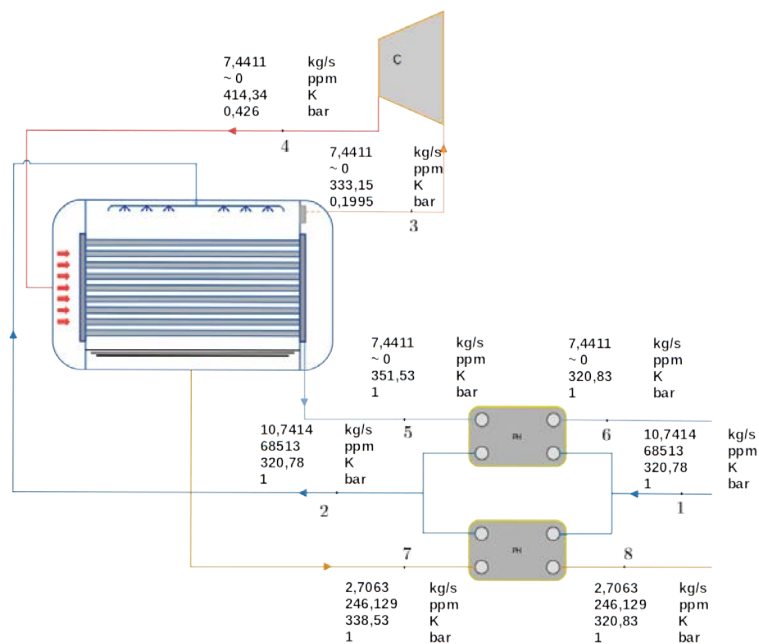


Figure 2.2: Process Flowsheet

The system considered in this work is a Single-Effect Mechanical Vapor Compression. The process flow diagram is illustrated below in Fig 1.4. The system includes the following components: the evaporator/condenser (EC), a mechanical compressor, brine and distillate preheaters, circulation pumps and venting system (which are not considered here for simplicity). Compressor and evaporator form a single unit. The two preheaters are used to recover the available heat in effluent streams (5 – 6 and 7 – 8). The feed water enters at ambient temperature and pressure ( $T_{f,1}, p_{f,1}$ ) and it is then split in two streams before entering the preheaters, of plate and frame type. Here, the incoming flow is heated thanks to the the sensible heat carried by the products (distillate and near-to-saturation brine) leaving the evaporator. The related temperature increase of the feed is important in terms of energy recovery of the system and consequently of plant efficiency. After the preheating, the feed brine enters the shell and tube EC and it is sprayed over the horizontal tube bundle through nozzles. There is a little increase in temperature of the subcooled liquid and once the brine saturation temperature ( $T_b$ ) has been reached, evaporation takes place. The change phase occurs below the atmospheric pressure, al-



lowing evaporation to take place at lower temperature than the saturation temperature at ambient pressure. The formed vapor passes through the demister and goes into a centrifugal compressor which is used to enhance the saturation pressure of the steam and superheat it. The superheated steam exiting the compressor flows inside the tubes of the condenser. At first it releases sensible heat reaching its saturation condition  $(T_d, p_d)$ , and then it condenses yielding the latent heat to the evaporating brine that covers the outside surface of the tubes. At the end of the phase change, the condensed water vapor and the brine come out from the vessel and goes into the preheaters to heat up the feed.



# Chapter 3

## Methods

The methodology used to evaluate the capital and operating expenditure as well as performance variables of the single effect mechanical vapor compression desalination system, is based on the development of three models combined together in a single integrated procedure. The mathematical models are developed in Matlab<sup>®</sup>. The starting point of the analysis is a brackish water sample, supplied by Lenntech B.V.. The first model predicts the BPE. Pitzer's equations represent a reliable choice, and they are used to evaluate colligative properties of brackish water and its concentrates. A thermodynamic design model of the thermal desalination process is then developed in order to obtain the performance variables along with the main inputs to the economic model. Finally, an economic model based on the module costing technique is developed, and employed to turn system performance variables into an economic value, taking into account materials of construction and operating conditions of the system.

### 3.1 Electrolytes solutions thermodynamics - Pitzer model

The properties of a mixture that depend only on the number of solutes (i.e. concentration), and not on their nature, are called colligative. This definition is not valid when the solutions are of high ionic strength and their behaviour cannot be described as ideal. In this case, it is necessary to adjust colligative properties using the osmotic coefficient ( $\phi$ )

Table 3.1: BWRO reject quality

| Constituent            |             | Concentration, <i>mg/L</i> |
|------------------------|-------------|----------------------------|
| Name                   | Symbol      |                            |
| Ammonium               | $NH_4^+$    | 0.00                       |
| Potassium              | $K^+$       | 327.99                     |
| Sodium                 | $Na^+$      | 16450.98                   |
| Magnesium              | $Mg^{2+}$   | 4652.18                    |
| Calcium                | $Ca^{2+}$   | 1813.68                    |
| Strontium              | $Sr^{2+}$   | 0.00                       |
| Barium                 | $Ba^{2+}$   | 0.00                       |
| Carbonate              | $CO_3^{2-}$ | 33.48                      |
| Bicarbonate            | $HCO_3^-$   | 698.38                     |
| Nitrate                | $NO_3^-$    | 3.15                       |
| Chloride               | $Cl^-$      | 41561.77                   |
| Fluoride               | $F^-$       | 4.30                       |
| Sulfate                | $SO_4^{2-}$ | 576.45                     |
| Carbon Dioxide         | $CO_2$      | 13.28                      |
| Silica                 | $SiO_2$     | 72.71                      |
| Boron                  | $B$         | 3.26                       |
| Total Dissolved Solids |             | 66213.72                   |

which quantifies the deviation of a solvent from the ideal behaviour. In thermal desalination processes, the boiling point elevation is the colligative property of interest (it is the difference between the saturation temperatures of a solution and that of its pure solvent). The exact vapor flow rate due to evaporation depends on the raising of boiling temperature (The exact vapor flow rate due to evaporation depends on the boiling temperature, and in turn on the salinity (at given heat flow rate). Higher boiling temperatures deriving higher salinity reduce the vapour flow rate at given heat flow rate). Therefore, an ion-interaction model is required to predict the osmotic coefficient of the water, which depends on the solutes' concentrations. The Pitzer model is chosen to achieve the purpose (equations in Appendix A). It starts from a virial expansion of the excess free energy of a solution

$$\frac{G_{ex}}{RT} = n_w [f(I) + \sum_i \sum_j \lambda_{ij}(I) m_i m_j + \sum_i \sum_j \sum_k \mu_{ijk} m_i m_j m_k] \quad (3.1)$$

where  $\phi$  is the aforementioned osmotic coefficient and  $m_i$  are molalities of each solute.

In order to obtain the expression of the osmotic coefficient, it is necessary to take the derivative of Eq. (1) with respect to the number of moles of the solvent (water) (the model calculates also the derivatives of Eq. (1) with respect to the number of moles of each component to evaluate their activities, but these are not of interest for the present analysis). Once the osmotic coefficient is obtained, it is easy to find the BPE using the following expression:

$$BPE = T_{sat} - T_{sat}^{\circ} = \frac{R T_{sat}^{\circ 2}}{r_{ev}^{\circ}} \phi \sum_i m_i \quad (3.2)$$

where  $R$  is the molar gas constant,  $r_{ev}$  and  $T_{sat}^{\circ}$  are the enthalpy of vaporization and the saturation temperature of pure water, respectively, while  $T_{sat}$  is the saturation temperature of the solution at fixed pressure. In most of the works concerning thermal desalination plants, interpolating relationships (given for different solution compositions) are used to find the BPE. Here it is evaluated starting from a representative water analysis (Table 1) of the rejected brine of a reverse osmosis process. Considering the composition of this sample, sodium and chloride represent most of the dissolved solids (more than 90%), and about 95% of the solutes are given by Na-Cl-Mg. All the other components are globally present as less than 5%. Although the other components may influence the system design through, e.g., scaling considerations, they do not affect the separation energy significantly [6]. Given the high percentage of NaCl, in this work, the aforementioned ternary system is considered as NaCl-equivalent (i.e., Mg is converted into NaCl according to the ratio of molar masses). In relation to scale formation this choice is conservative. Indeed, precipitation of sodium chloride is the main concern in the system, although additional pretreatments for brackish water sources are often required to mitigate the effects of silica and nitrates.

## 3.2 Thermodynamic model of the MVC brine minimization system

The assumptions used to develop the thermodynamic model of the single effect MVC thermal desalination plant are:

1. Steady state operations,
2. The driving force for heat transfer in the evaporator is assumed constant and equal to the difference between the condensation and evaporation temperatures,
3. The latent heats of formed vapor and condensing steam are temperature dependent,
4. The heat capacities for brine and distillate depend on temperature and composition,
5. The specific heat of the superheated vapor is constant and considered at the average temperature,
6. The preheaters have different heat transfer areas
7. The effluent heating streams have the same temperature ( $T_0$ ),
8. The Overall heat transfer coefficient in the preheaters is constant, but not equal,
9. The distillate concentration is assumed to be equal to 0 *ppm*,
10. The effect of the boiling point elevation is included in calculations,
11. The temperature losses related to the demister and the NEA are neglected.

The main input variables are shown in Table 2. The model can predict the variables of interest for the economical evaluation. The working fluid is assumed to be pure aqueous sodium chloride. The model to be solved follows a sequential-modular approach.

Table 3.2: Independent variables

| Main system specifications |           |                   |
|----------------------------|-----------|-------------------|
| $c_f$                      | 68513.329 | $\frac{mg}{L}$    |
| $p_{f,1}$                  | 1         | <i>bar</i>        |
| $T_{f,1}$                  | 298.15    | <i>K</i>          |
| $\dot{V}_f$                | 35        | $\frac{m^3}{h}$   |
| $M_{NaCl}$                 | 58.4428   | $\frac{g}{mol}$   |
| $\gamma$                   | 1.33      | /                 |
| $\eta_{is}$                | 0.85      | /                 |
| $\Delta T$                 | 10        | <i>K</i>          |
| $T_{ev}$                   | 333.15    | <i>K</i>          |
| $U_{ev}$                   | 3.0       | $\frac{kW}{m^2K}$ |
| $RR_{ev}$                  | 73.33     | %                 |

In order to reach the purpose mass (3.3) and energy (3.4) balances are performed for each component of the system, at steady-state conditions.

$$0 = \sum_i \dot{m}_i - \sum_e \dot{m}_e \quad (3.3)$$

$$0 = \dot{Q} - \dot{W} + \sum_i \dot{m}_i h_i - \sum_e \dot{m}_e h_e \quad (3.4)$$

in which  $\dot{m}_i$  and  $\dot{m}_e$ , are mass flowrates, at inlet and outlet of the control volume respectively.  $\dot{Q}$  and  $\dot{W}$  represent net rates of heat and work, while  $\dot{m}_i h_i$  and  $\dot{m}_e h_e$  stand for enthalpy rates through system boundary. The terms to the left of the previous balances represent the differentials with respect to time of mass and energy in consideration of the control volume. As regards to the control volume comprising the evaporator and the compressor, the concentration process is also described by the salt balance (3.5):

$$\dot{m}_i x_i = \sum_e \dot{m}_e x_e \quad (3.5)$$

where  $x_i$  and  $x_e$  are mass concentrations of inlet and outlet streams. The outlet streams are respectively the rejected brine and the distillate. The model calculates temperature, pressure, mass flow rate and salinity in each point of the system. Moreover, thanks to the correlations of heat transfer (illustrated in Appendix B), the area required by heat exchangers can be calculated. Regarding the compressor, an isentropic model is implemented to allow an estimation of power consumption in the system. Thermophysical properties are evaluated at the average temperature during sensible heat exchanges. With regards to aqueous-NaCl, density and specific heat ( $\rho$ ,  $c_p$ ) are estimated in function of temperature and salinity and can be found in literature [11]. In relation to the calculation of the density, concentration (on mass basis) should be hypothesized to perform the required iteration in order to find the value. The latent heats of condensation and evaporation ( $r_c$  and  $r_{ev}$ ), and the enthalpy values of saturated liquid water ( $h_d$ ,  $h_0$ ) are calculated through correlations in function of the temperature [2]. The specific heat of the superheated vapor is evaluated at the saturation pressure ( $p_d$ ) and medium temperature between the superheated and condensation conditions. Saturation pressure and temperature are evaluated through a Matlab tool based on [15]. Thus, discharge temperature values from the preheaters (both equal to  $T_0$ ) and the temperature of the feed input to the evaporator ( $T_{f,2}$ ) need to be initially assumed to be able to evaluate the

values through the iteration process using the Newton-Raphson method. The global heat transfer coefficients of the preheaters ( $U_d$  and  $U_b$ ) are estimated as a function of temperature [2], while the global heat transfer coefficient of the evaporator ( $U_{ev}$ ) is chosen as a fixed value. The isentropic efficiency ( $\eta_{is}$ ) of the compressor and the specific heat ratio of the vapor ( $\gamma$ ) are considered as independent variables. It is necessary to select the saturation temperature of pure water ( $T_{ev}$ ) and the driving force of the heat transfer ( $\Delta T$ ), which is understood as the difference between the boiling brine temperature and the condensing vapor temperature. The recovery ratio of the evaporator is chosen to be 73.33%. When the calculation of the thermodynamic quantities of the cycle is completed, areas of heat exchangers and power consumption of the compressor are known. These variables are needed by the economic model to complete the analysis.

### 3.3 Economic model

Table 3.3: Economic Parameters

| Main Economic Parameters                   |       |
|--|-------|
| Electricity cost, $\text{€}KW h_{el}^{-1}$ | 0.12  |
| Interest rate, %                           | 5     |
| Average personal cost, $\text{€}y^{-1}$    | 50000 |
| Pure water cost, $\text{€}L^{-1}$          | 2     |
| Amortization period, $y$                   | 10    |

The economic model receives as input parameters the main outputs of the technical model, i.e. the areas of the shell and tube EC, the preheaters and the work required by the compressor. All the relevant parameters used for the economic model are reported in Table 3.3. The outputs of the economic model are fixed and operating cost, as well as the Total annualized Cost (TAC).

#### 3.3.1 Fixed Costs

The module costing technique is used to evaluate the fixed costs of the components of the system. This technique, which is widely described in [14], suggests that the cost



of generic equipment (Bare Module Cost,  $C_{BM}$ ) is related to the purchased cost of the equipment ( $C_p^0$ ) assessed for certain standard conditions, such as ambient pressure and common materials. With the purpose of taking in consideration deviations from the base case, some correction factors, related to the construction materials and the operating pressure, are included in the Bare Module Factor ( $F_{BM}$ ). In particular the  $F_M$  and  $F_P$  factors have to be considered for different materials and pressures with respect to the base case. The  $C_p^0$  is calculated in function of the component size and then actualized via the Chemical Engineering Plant Cost Index (CEPCI, 2017). Eventually, the bare module cost of the equipment is calculated multiplying the purchased cost of the equipment by the bare module factor, as in (3.6).

$$C_{BM} = C_p^0 F_{BM} \quad (3.6)$$

When talking about the evaporator, it is supposed to have the shell in carbon steel and the tubes in a nickel-based alloy, which has an excellent resistance to corrosion from saltwater at high temperatures. The preheaters materials are chosen to be Nickel alloy as well, and the compressor to be built in carbon steel. The total cost of the equipment is calculated as the sum of the costs of the single effect, plus the cost of the two preheaters and the compressor. Finally, the total module cost ( $C_{TM}$ ) is evaluated adding the contingency and fee cost to the cost of equipment, which are defined as 15% and 3% of the cost of equipment, respectively. The auxiliary facility cost is neglected. The total module cost is annualized (CAPEX in  $\text{k€y}^{-1}$ ), through the interest rate ( $i$ ) and assuming a certain plant amortization period ( $n_{years}$ ), according to (3.7), where the second term is defined as the *factor of annualization* for the capital investment *fac*.

$$CAPEX = C_{TM} \frac{(1+i)^{n_{years}} i}{(1+i)^{n_{years}} i} \quad (3.7)$$

### 3.3.2 Operating Costs

The operating costs take into account maintenance and labor costs, personnel costs and electric energy costs. The maintenance cost is estimated as the 3% of the CAPEX (on an annual basis), while the labor cost for maintenance is defined as the 20% of the personnel

cost [15]. This last term is given by the average cost of the personal multiplied by the number of required workers. The electric energy cost is calculated multiplying the specific electric consumption (calculated and equal to  $1.5 \text{ kWhel m}^{-3}$ ) by the electricity cost (European, 2017). Finally the thermal energy cost is not considered in this work, and it would be referred only for the start up process. The distillate is a by-product which can be sold, thus the revenue relevant to the produced distillate is subtracted from the operating costs. The total annual operating cost (OPEX in  $\text{k€y}^{-1}$ ) is given by the sum of all the described operating cost terms.

# Chapter 4

## Results

The present work is focused on the investigation of a mechanical vapor compressor system performances within the treatment of the high salinity effluent produced in a brackish water RO process. The results come together taking in consideration that the feed mixture is modelled as pure aqueous-NaCl. The feed water flow rate is  $35 \frac{m^3}{h}$  at a concentration of  $68513.329 \frac{mg}{L}$ . The system operates at a recovery ratio of 73.33%, with a fresh water production of  $7.4411 \frac{kg}{s}$  and a brine concentration reaching almost  $250 \frac{g}{kg}$ . The recovery ratio of the thermal process has to be high enough to discharge brine at near saturation conditions. In addition, it is required a compressor with 1010.406 kW of capacity. The isentropic efficiency of 0.85, while the specific work is of  $37.722 \frac{kWh_{el}}{kg_d}$  (or  $135.787 \frac{kW}{kg_d s^{-1}}$ ). The work of the compressor is needed to enhance the pressure from 0.1995 bar (at which corresponds an evaporation temperature of pure water of 333.15 K and a boiling point elevation of 5.3767 K) to 0.3921 bar (corresponding to the condensation temperature of vapor of 348.5667 K). The distillate and brine preheaters require respectively  $14.658 m^2$  and  $4.124 m^2$  heat transfer areas. The specific heat transfer area (id est the area of all heat exchangers needed to produce  $1 \frac{kg}{s}$  of pure water) is of  $83.519 \frac{m^2}{kg_d s^{-1}}$ , while the specific heat transfer area of the evaporator is of  $80.995 \frac{m^2}{kg_d s^{-1}}$ . As regard to the evaporator the required heat duty is of 18080.61 kW. It takes a specific heat duty of  $2429.83 \frac{kW}{kg_d s^{-1}}$ . The capital and operational expenditures at the design point are respectively equal to 1119.7 k€y<sup>-1</sup> and 641.1 k€y<sup>-1</sup>, for a comprehensive total annualized cost of 1760.8 k€y<sup>-1</sup>.

The variation of the boiling point elevation with molality and temperature is shown in Fig 1.3. It is easy to see how temperature differences do not affect too much its value; on

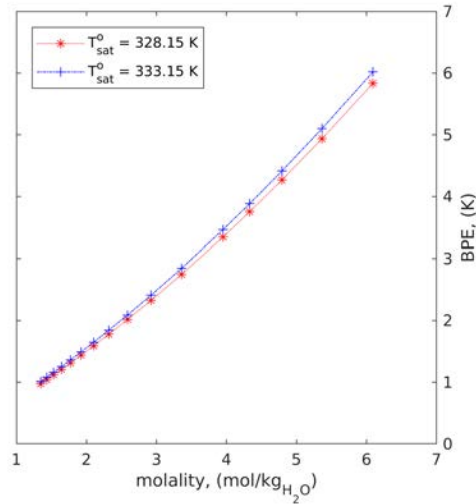


Figure 4.1: Influence of molality and temperature on the Boiling Point Elevation.

the contrary the contribution of molality (and therefore salinity) is not small. Although for seawater processes the boiling point elevation (BPE) is relatively small, for brine volume minimization purposes it can assume larger values which lead to a major energy consumption of the process.

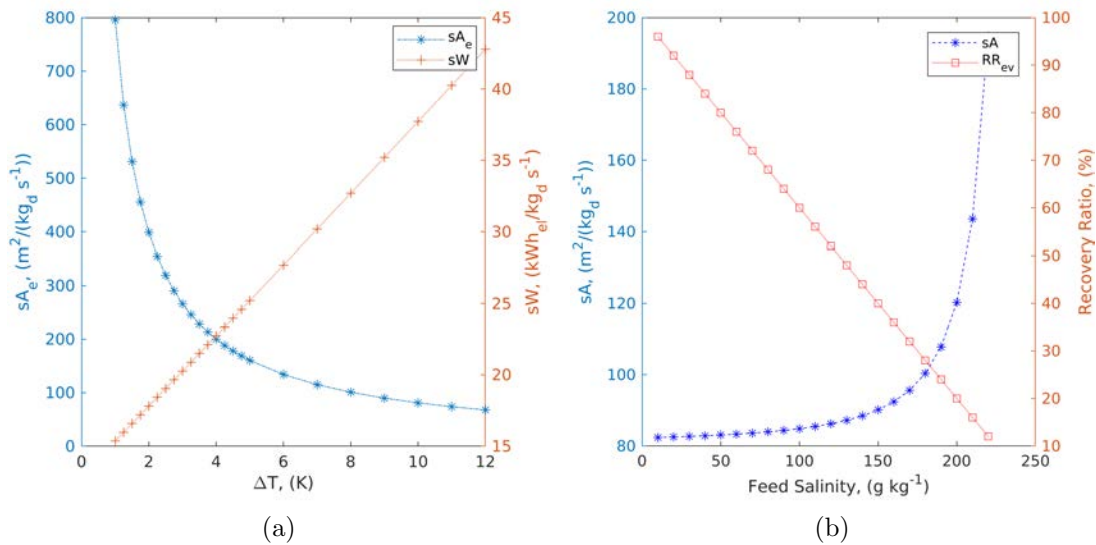


Figure 4.2: (a) Influence of the temperature difference on the specific power consumption and the heat transfer area. (b) Comparative effect of produced water salinity on the specific heat transfer area and recovery ratio.

The system behaviour is studied varying the main design variables. Fig 1.4a) shows how the specific heat transfer area of the evaporator ( $sA_e$ ) and the specific power consumption

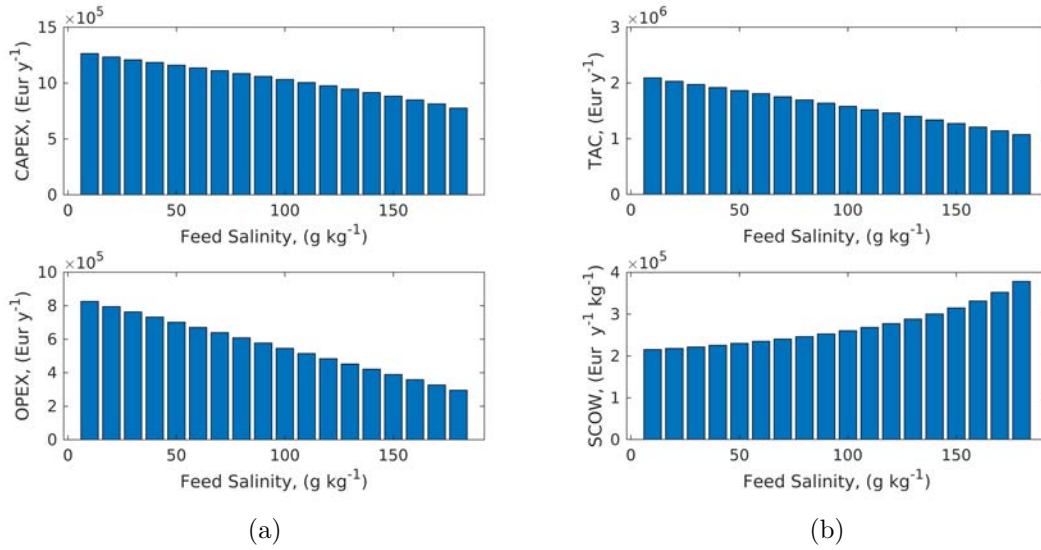


Figure 4.3: (a) Effect of increasing the salinity of feed water on capital and operational expenditure. (b) Effect of increasing the salinity of feed water total annualized cost and simplified cost of water.

of the compressor ( $sW$ ) vary with the temperature difference between the condensing vapor and the boiling brine ( $\Delta T$ ). It is important to note the importance of this parameter from an economic point of view. In fact, in this type of application in which the feed is highly corrosive, materials selection of the tubes brings to choose their construction in Nickel or in Titanium which are expensive. Figure 1.4b) shows the effects of the increasing feed flow salinity, while fixing the discharge brine salinity at  $250 \frac{g}{kg}$ , on the recovery ratio and the specific heat transfer area of the heat exchangers. It leads to a reduction in the recovery rate as the production of fresh water decreases leading to the specific increase in the heat transfer area. As regard to Fig 2.1 it is interesting to note that by fixing the concentration of the brine, both curves of the capital and operational expenditure decrease (and consequently the total annualized cost in Fig 2.1b)) as the salinity of the feed water increases. This fact is due to the smaller equipment size, and the consequent lower for energy consumption. In the end Fig 2.1b) shows how the simplified cost of water (defined as the ratio between the sum between CAPEX and OPEX and the product distillate) increases as the salinity of the feed water increases.



# Chapter 5

## Conclusions

An integrated procedure to design thermal desalination systems based on mechanical vapor compression has been developed. The models are applied to a real case for the evaluation of capital and operational expenditures for the selected technology. The model is based on previous developed models, and the values obtained in a near saturation conditions are in line with those obtained in similar works [17] and the ones of the market. It is therefore considered that the model can be a useful tool for the economic evaluation of other similar works. The effect of salinity is investigated versus the main economical variables, showing how the mechanical vapor compressor system is a very suitable technology to treat harsh feed waters, which is in accordance with [6]. The feed flow rate is  $10.147 \frac{kg}{s}$  at a concentration of almost  $70 \frac{g}{kg}$  and considering a recovery ratio of 73.33% the fresh water flow rate is of  $7.441 \frac{kg}{s}$  and the TDS of the discharged brine is approximately of  $250 \frac{g}{kg}$ . Finally, capital and operational expenditure are respectively evaluated as  $1119.7 \text{ k€y}^{-1}$  and  $641.1 \text{ k€y}^{-1}$ .





# Appendix A

## Pitzer equations and parameters

The model is a system of equations useful to predict electrolyte thermodynamic properties, introduced by K.S.Pitzer since 1973. In order to achieve the purpose the Pitzer's approach begins with a virial expansion of the excess free energy (the actual free energy minus the one of an ideal solution of the same composition).

$$\frac{G_{ex}}{RT} = n_w [f(I) + \sum_i \sum_j \lambda_{ij}(I) b_i b_j + \sum_i \sum_j \sum_k \mu_{ijk} b_i b_j b_k] \quad (\text{A.1})$$

where  $n_w$  is kilograms of water and  $m_i$  is molality of solute  $i$ ;  $R$  is the molar gas constant and  $T$  is the thermodynamic temperature.  $f(I)$  represents the Debye-Hückel term and it is a function of only ionic strength  $I = \frac{1}{2} \sum_i b_i z_i^2$ , namely the electric field strength in an electrolyte solution. The second and third virial coefficients, respectively  $\lambda_{ij}$  and  $\mu_{ijk}$ , take in account for the short range potential effects between solute pairs and triplets (where the second term is not relevant in this work, as it is considered only NaCl). Derivatives of (A.1) with respect of the number of moles of each of the components bring to three main equations representing the osmotic coefficient  $\phi$  and the activity coefficients for anions and cations,  $\gamma_X$  and  $\gamma_M$  respectively. The following model, (A.2) to (A.12) refer to binary aqueous electrolytes systems, and in particular for aqueous-NaCl.

$$(\phi - 1) = \frac{\frac{\partial G_{ex}}{\partial n_w}}{RT \sum_i m_i} = \frac{2}{\sum_i m_i} \left[ \frac{-A^\phi I^{3/2}}{1 + 1.2\sqrt{I}} + \sum_c \sum_a m_c m_a (B_{ca}^\phi + ZC_{ca}) \right] \quad (\text{A.2})$$

$$\ln \gamma_M = \frac{1}{RT} \frac{\partial G_{ex}}{\partial m_M} = z_M^2 F + \sum_a m_a (2B_{Ma} + ZC_{Ma}) + |z_M| \sum_c \sum_a m_c m_a C_{ca} \quad (\text{A.3})$$

$$\ln \gamma_X = \frac{1}{RT} \frac{\partial G_{ex}}{\partial m_X} = z_X^2 F + \sum_c m_c (2B_{cX} + ZC_{cX}) + |z_X| \sum_c \sum_a m_c m_a C_{ca} \quad (\text{A.4})$$

In the above equations,  $Z = \sum_i m_i |z_i|$ , the subscripts  $M$  and  $c$  refer to cations while  $X$  and  $a$  are anions and  $i$  refers to all the solutes in the solution; the  $m$  terms denotes their molal concentration ( $mol/kg_{solvent}$ ), and  $z$  represents the charge. The summation indexes  $a$ ,  $c$  and  $i$ , denotes the sum over all anions, cations and solutes in the system. As mentioned before, K.S.PITZER (1973) in his model assumed functional forms of  $\lambda_{ij}(I)$ . They are represented by  $B$ 's and  $\Phi$ 's terms showed in (A.2) to (A.4). Regarding (A.3) and (A.4), the  $F$  term is mathematically defined as showed below.

$$F = -A^\phi \left[ \frac{\sqrt{I}}{1 + 1.2\sqrt{I}} + \frac{2}{1.2} \ln 1 + 1.2\sqrt{I} \right] + \sum_c \sum_a m_c m_a B'_{ca} \quad (\text{A.5})$$

The  $A^\phi$  term above is related to the Debye-Hückel limiting law and it is given by

$$A^\phi = \frac{1}{3} \left[ \frac{e^3 (2N_0 \rho_w)^{\frac{1}{2}}}{8\pi (\epsilon_r \epsilon_0 k_b T)^{\frac{3}{2}}} \right] \quad (\text{A.6})$$

where  $\rho_w$ ,  $\epsilon_r$  are respectively the density and the relative permittivity of water, which are evaluated with correlations available in ([17, 18]);  $e$  is the electron charge,  $N_0$  is the Avogadro's number and  $k_b$  is the Boltzmann constant.  $T$  is the absolute temperature, and despite it plays a role in variations of every binary adjustable parameter ( $\beta_{MX}^{(i)}$ ,  $C_{MX}^\phi$ ),  $A^\phi$  is the most influenced term regarding the activity coefficients computation. Functions  $B_{ij}$ ,  $B'_{ij}$ ,  $B_{ij}^\phi$  and  $C_{ij}$  represent interactions between anions and cations and the parameters  $\beta_{MX}^{(i)}$  and  $C_{MX}^\phi$  are tabulated for every given ion pair. In particular,  $\beta_{MX}^{(2)}$  is relevant only for 2-2 electrolytes, in which case  $\alpha_1 = 1.4$  and  $\alpha_2 = 12$ . For 1-j type of electrolyte usually disappear the last term of (A.7) to (A.9) and  $\alpha_1 = 2.0$ . The following functional forms, dependent by ionic strength, were chosen in order to fit experimental

data.

$$B_{MX}^\phi = \beta_{MX}^{(0)} + \beta_{MX}^{(1)}e^{-\alpha_1\sqrt{I}} + \beta_{MX}^{(2)}e^{-\alpha_2\sqrt{I}} \quad (\text{A.7})$$

$$B_{MX} = \beta_{MX}^{(0)} + \beta_{MX}^{(1)}g(\alpha_1\sqrt{I}) + \beta_{MX}^{(2)}g(\alpha_2\sqrt{I}) \quad (\text{A.8})$$

$$B'_{MX} = \beta_{MX}^{(1)}\frac{g'(\alpha_1\sqrt{I})}{I} + \beta_{MX}^{(2)}\frac{g'(\alpha_2\sqrt{I})}{I} \quad (\text{A.9})$$

$$C_{MX} = \frac{C_{MX}^\phi}{2\sqrt{|z_M z_X|}} \quad (\text{A.10})$$

Here  $B'_{MX}$  is the derivative of  $B_{MX}$  with respect to the ionic strength, and functions  $g$  and  $g'$  are defined as

$$g(x) = \frac{2[1 - (1+x)e^{-x}]}{x^2} \quad (\text{A.11})$$

$$g'(x) = \frac{-2[1 - (1+x + \frac{x^2}{2})e^{-x}]}{x^2} \quad (\text{A.12})$$

# Appendix B

## Thermodynamic model - Single Effect Mechanical Vapor Compression system

With referement to the flowsheet shown in Fig 1.2, mass balances, energy balances and performance parameters of every component will be shown.

### Preheaters Design

#### *Mass Balances*

$$\dot{m}_{f_1} = \dot{m}_{f_2} = \dot{m}_f \quad (\text{B.1})$$

$$\dot{m}_{b,3} = \dot{m}_{b,4} = \dot{m}_b \quad (\text{B.2})$$

$$\dot{m}_{d,5} = \dot{m}_{d,6} = \dot{m}_d \quad (\text{B.3})$$

#### *Energy Balance*

$$\dot{m}_{f,1} c_{p_{f1}} (T_{f_2} - T_{f_1}) = \dot{m}_d (h_d - h_0) + \dot{m}_b c_{p_b} (T_b - T_0) \quad (\text{B.4})$$

## Distillate Preheater

$$\dot{m}_d(h_d - h_0) = A_d U_d \Delta T_{ml_d} , \quad (\text{B.5})$$

$$\Delta T_{ml_d} = \frac{(T_d - T_{f_2}) - (T_0 - T_{f_1})}{\ln\left(\frac{T_d - T_{f_2}}{T_0 - T_{f_1}}\right)} \quad (\text{B.6})$$

## Brine Preheater

$$\dot{m}_b c_{p_b} (T_b - T_0) = A_b U_b \Delta T_{ml_b} , \quad (\text{B.7})$$

$$\Delta T_{ml_b} = \frac{(T_b - T_{f_2}) - (T_0 - T_{f_1})}{\ln\left(\frac{T_b - T_{f_2}}{T_0 - T_{f_1}}\right)} \quad (\text{B.8})$$

## Evaporator Design

### *Mass and Salt Balances*

$$\dot{m}_f = \dot{m}_b + \dot{m}_d \quad (\text{B.9})$$

$$\dot{m}_f x_f = \dot{m}_b x_b \quad (\text{B.10})$$

### *Energy Balance*

$$\dot{m}_{f,2} c_{p_f} (T_b - T_{f_2}) + \dot{m}_d r_e = \dot{m}_d r_c + (h_d - h_0) + \dot{m}_d c_{p_s} (T_s - T_d) \quad (\text{B.11})$$

$$\dot{m}_d c_{p_s} (T_s - T_d) + \dot{m}_d r_c = A_e U_e (T_d - T_b) \quad (\text{B.12})$$

## Compressor Design

The compressor is designed as an isentropic process.

### *Mass Balance*

$$\dot{m}_{d,7} = \dot{m}_{d,8} \quad (\text{B.13})$$

*Energy balance*

$$\dot{W} = (h_{d8} - h_{d7}) \quad (\text{B.14})$$

$$T_{is} = T_s \left( \frac{p_d}{p_{ev}} \right)^{\frac{\gamma-1}{\gamma}} \quad (\text{B.15})$$

$$T_s = \frac{(T_{is} - T_{ev})}{\eta_{is}} + T_{ev} \quad (\text{B.16})$$

# Bibliography

- [1] A. Giwa, V. Dufour, F. Al Marzooqi, M. Al Kaabi, and S. W. Hasan. *Brine management methods: Recent innovations and current status*. Desalination, vol. 407, pp. 1–23, 2017.
- [2] H. T. El-Dessouki, H. M. Ettouney. *Fundamentals of Salt Water Desalination*. Elsevier, 2002. 19, 20
- [3] H. M. Ettouney. *Design of single-effect mechanical vapor compression*. Desalination 190 (2006), 1-15. doi:10.1016/j.desal.2005.08.003
- [4] K. S. Pitzer. *Thermodynamics of Electrolytes. I. Theoretical Basis and General Equation*. The Journal of Physical Chemistry, vol. 77, No. 2, 1973.
- [5] K. S. Pitzer and G. Mayorga. *Thermodynamics of Electrolytes. II. Activity and Osmotic Coefficients for Strong Electrolytes with One or Both Ions Univalent*. The Journal of Physical Chemistry, vol. 77, no. 19, pp. 2300–2308, 1973.
- [6] Gregory P. Thiel, Emily W. Tow, Leonardo D. Banchik, Hyung Won Chung, John H. Lienhard V. *Energy consumption in desalinating produced water from shale oil and*. Desalination 366 (2015) 94–112. <http://dx.doi.org/10.1016/j.desal.2014.12.038>  
27
- [7] Gregory P. Thiel, John H. Lienhard V. *Treating produced water from hydraulic fracturing: Composition effects on scale formation and desalination system selection*. Desalination 346 (2014) 54–69. <http://dx.doi.org/10.1016/j.desal.2014.05.001>
- [8] Karan H. Mistry, Harrison A. Hunter, John H. Lienhard V. *Effect of composition and nonideal solution behavior on desalination calculations for mixed elec-*

- trolyte solutions with comparison to seawater.* Desalination 318 (2013) 34–47.  
<http://dx.doi.org/10.1016/j.desal.2013.03.015>
- [9] Karan H. Mistry, Ronan K. McGovern, Gregory P. Thiel, Edward K. Summers, Syed M. Zubair and John H. Lienhard V. *Entropy Generation Analysis of Desalination Technologies.* Entropy 2011, 13, 1829-1864. doi:10.3390/e13101829
- [10] Hyung Won Chung, Kishor G. Nayar, Jaichander Swaminathan, Karim M. Chehayeb, John H. Lienhard V. *Thermodynamic analysis of brine management methods: Zero-discharge desalination and salinity-gradient power production.* Desalination 404 (2017) 291–303. <http://dx.doi.org/10.1016/j.desal.2016.11.022>
- [11] A. Ramalingam, and S. Arumugam. *Experimental Study on Specific Heat of Hot Brine for Salt Gradient Solar Pond Application.* International Journal of ChemTech Research, Vol.4, No.3, pp. 956-961 (2012) 19
- [12] The International Association for the Properties of Water and Steam *Revised Release on the IAPWS Industrial Formulation 1997 for the Thermodynamic Properties of Water and Steam* Available at: <http://www.iapws.org/relguide/IF97-Rev.pdf>
- [13] Wolfgang Wagner, Hans-Joachim Kretzschmar. *International Steam Tables* Springer. Available at: <http://www.steamshed.com/pdf/017InternationalSteamTables.pdf>
- [14] R. Turton, R. C. Bailie, W. B. Whiting, J. A. Shaeiwitz, and D. Bhattacharyya. *Analysis, Synthesis and Design of Chemical Processes.* Prentice Hall. 20
- [15] T. Laukemann, F. Verdier, R. Baten, F. Trieb, M. Moser, and T. Fichter *MENA Regional Water Outlook, Phase II, Desalination using Renewable Energy* Fichtner and DLR, 2012. 19, 22
- [16] Viviani C. Onishi, Alba Carrero-Parreño, Juan A. Reyes-Labarta, Eric S. Fraga c, Jose A. Caballero. *Desalination of shale gas produced water: A rigorous design approach for zero-liquid discharge evaporation systems.* Journal of Cleaner Production 140 (2017) 1399-1414 <http://dx.doi.org/10.1016/j.jclepro.2016.10.012>



- [17] Daniel J. Bradley and Kenneth S. Pitzer *Thermodynamics of electrolytes. 12. Dielectric properties of water and Debye-Hueckel parameters to 350.degree.C and 1 kbar*. The Journal of Physical Chemistry 1979 83 (12), 1599-1603 DOI: 10.1021/j100475a009 27, 30
- [18] George S. Kell *Density, thermal expansivity, and compressibility of liquid water from 0.deg. to 150.deg.. Correlations and tables for atmospheric pressure and saturation reviewed and expressed on 1968 temperature scale*. Journal of Chemical Engineering Data 1975 20 (1), 97-105 DOI: 10.1021/je60064a005 30
- [19] A. Subramani, J.G. Jacangelo *Treatment technologies for reverse osmosis concentrate volume minimization: A review*. Separation and Purification Technology 122 (2014) 472–489 <http://dx.doi.org/10.1016/j.seppur.2013.12.004> 5, 7
- [20] A. Giwa, V. Dufour, F. Al Marzooqi, M. Al Kaabi, S.W. Hasan *Brine management methods: Recent innovations and current status*. Desalination 407 (2017) 1–23 <http://dx.doi.org/10.1016/j.desal.2016.12.008> 7, 10
- [21] F. Rodríguez-DeLaNuez, N. Franquiz-Suárez, D.E. Santiago, J.M. Veza, J.J. Sadhwani, *Reuse and minimization of desalination brines: a review of alternatives*. Desalin. Water Treat. 39 (2012) 137–148 <http://dx.doi.org/10.1080/19443994.2012.669168>. 5, 7
- [22] L.F. Greenlee, D.F. Lawler, B.D. Freeman, B. Marrot, P. Moulin *Reverse osmosis desalination: water resources, technology, and today's challenges*. Water Res. 43 (2009) 2317–2328 5
- [23] Shefaa Mansour, Hassan A. Arafat, Shadi W. Hasan *Brine Management in Desalination Plants*. Desalination Sustainability: Chapter Five, (2017) 207-236 <http://dx.doi.org/10.1016/B978-0-12-809791-5.00005-5> 5
- [24] D.H. Kim *A review of desalting process techniques and economic analysis of the recovery of salts from retentates*. Desalination 270 (2011) 1–8. 10

- [25] M.J. Fernández-Torres, D.G. Randall, R. Melamu, H. von Blottnitz, *A comparative life cycle assessment of eutectic freeze crystallization and evaporative crystallization for the treatment of saline wastewater*. Desalination 306 (2012) 17–23 10
- [26] D.G. Randall, J. Nathoo, A.E. Lewis *A case study for treating a reverse osmosis brine using eutectic freeze crystallization – approaching a zero waste process*. Desalination 266 (2011) 256–262 10
- [27] Entropie, Veolia *Multiple Effect Distillation, The Technology*.  
<http://www.entropie.com/en/services/desalination/MEDj>, 6
- [28] G.P. Narayan and J.H. Lienhard V. *Humidification dehumidification desalination*. In J. Kucera, editor, Desalination: Water from Water, Chapter 9, pages 425–472 8
- [29] C. Kazner, S. Jamil, S. Phuntsho, H.K. Shon, T. Wintgens, S. Vigneswaran *Forward osmosis for the treatment of reverse osmosis concentrate from water reclamation: process performance and fouling control*. Water Sci. Technol. 69 (2014) 2431–2437  
<http://dx.doi.org/10.2166/wst.2014.138>. 9
- [30] B.B. Ashoor, S. Mansour, A. Giwa, V. Dufour, S.W. Hasan *Principles and applications of direct contact membrane distillation (DCMD): a comprehensive review*. Desalination 398 (2016) 222–246, <http://dx.doi.org/10.1016/j.desal.2016.07.043> 9
- [31] L.M. Camacho, L. Dumée, J. Zhang, J. De Li, M. Duke, J. Gomez, et al. *Advances in membrane distillation for water desalination and purification applications*. Water (Switzerland) 5 (2013) 94–196 <http://dx.doi.org/10.3390/w5010094> 9